Enabling feedback position control of an industrial robot based on external sensor signals for dual-stage actuation

Matthias Laimer, Daniel Wertjanz, Peter Gsellmann, Georg Schitter, and Ernst Csencsics
Automation and Control Institute
Technische Universität Wien
Vienna, Austria
laimer@acin.tuwien.ac.at

***Abstract*—This paper presents an advanced control error processing to enable the feedback position control of an industrial robot based on external sensor signals for dual-stage actuation. A measurement module comprising a magnetically levitated platform with an integrated 3D measurement tool is mounted as end effector on the industrial robot. The industrial robot is used to maintain the measurement platform within its limited actuation range, while actively tracking a sample in motion. The measurement module provides the short stroke but precision positioning of the measurement tool relative to a sample surface in 6-DoF. For a feedback controlled repositioning of the industrial robot's tool center point based on the internal measurement platform's position signals, a real-time interface is used. The implementation of the advanced control error processing successfully demonstrates the active tracking of a sample in motion, with residual tracking errors of 473 nm rms in sample-motion direction.**

***Index Terms*—Mechatronics, inline tracking systems, dual stage-actuation**

I. Introduction

An important aspect of remaining competitive in modern industrial manufacturing is the constant increase in product quality, which goes hand in hand with a continuous raise of the production efficiency. [1]. A key aspect of keeping pace with these trends is a flexible, resource-efficient and fast industry that can react quickly to varying market requirements [2], [3]. In this context, inline measuring systems are seen as a key factor for the production of the future, as they enable 100 % quality control while at the same time increasing product reliability and continuous monitoring of the production process, allowing the manufacturing procedure to be optimized in real time [2], [4]. Due to the growing need for automation for quality evaluation in manufacturing [5], there has been a substantial rise in the use of industrial robots (IRs) for inspection duties over the past few years [6], [7].

With constantly increasing the product quality, high-precision manufacturing systems, such as it is required for the production of optical systems and stacked IC components, measuring precision in the single to sub-micrometer range are demanded [8], [9]. To enable such high-precision measurements, precise alignment of the measuring tool relative to the sample surface is required, which is why such measurements are often carried out in environments that are isolated from external vibrations [10]. With the objective of increasing production efficiency even further, the aim is to perform such high-precision measurements directly in the production line [11].

In this relation, robotic systems provide the required flexibility and versatility, and are fast enough to place a measurement tool at arbitrary sample surface locations, such as required for the inspection of free-form surfaces, e.g., in the automotive industry [12]. However, current robotic inline measurement systems achieve positioning precision of several tens of micrometers, which is mainly caused, due to the finite stiffness of IRs [7]. In addition, motion-related blur caused by environmental vibrations, e.g, production processes impair the achievable resolution of the measurements conducted directly in a production line even further [13]. Lately, research has focused on systems, which are able to create local lab-like conditions within the production line, by actively tracking the sample motion [14]. A magnetically levitated 3D measurement platform (MP) mounted as end effector to an IR has been proposed [15]. The measuring platform, in which a scanning confocal chromatic sensor (SCCS) is embedded as a 3D measuring tool, is mechanically decoupled from the IR and thus also from environmental disturbances by a quasi-zero stiffness actuation [16]. The relative motion in six degrees of freedom (DOFs) between the sample surface and the measurement tool is compensated, by enabling a contactless but stiff link by means of feedback control. To enable measurements on moving samples along arbitrary paths, it combines the long-range and flexible positioning capability of the IR with the short-stroke positioning range of the high-precision MP in a dual-stage actuation concept [17].

The contribution of this paper is the design of an advanced

The authors are with the Christian Doppler Laboratory for Precision Measurements in Motion, Automation and Control Institute (ACIN), Technische Universität Wien, 1040 Vienna. Corresponding author: laimer@acin.tuwien.ac.at

Pre-print version of the article: M. Laimer, D. Wertjanz, P. Gsellmann, G. Schitter, and E. Csencsics, "Enabling feedback position control of an industrial robot based on external sensor signals for dual-stage actuation," *2024 IEEE International Conference on Advanced Intelligent Mechatronics (AIM)*1252-1257, 2024. DOI: 10.1109/AIM55361.2024.10637010

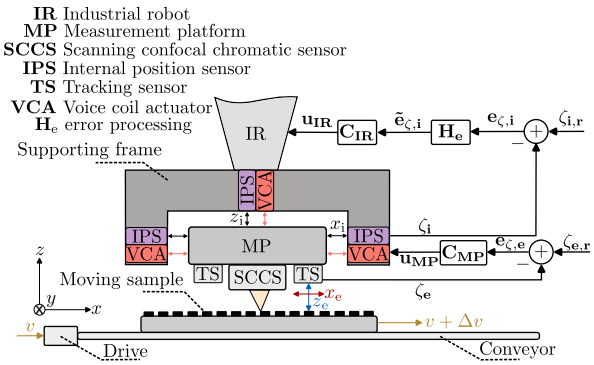

Fig. 1: Dual stage-controlled positioning system for precision measurements on moving samples. A constant relative position x_e and z_e between the MP and sample is maintained by the feedback controller $\mathbf{C_{MP}}$. The feedback controller $\mathbf{C_{IR}}$ repositions the IR based on the internal MP positions x_i and z_i.

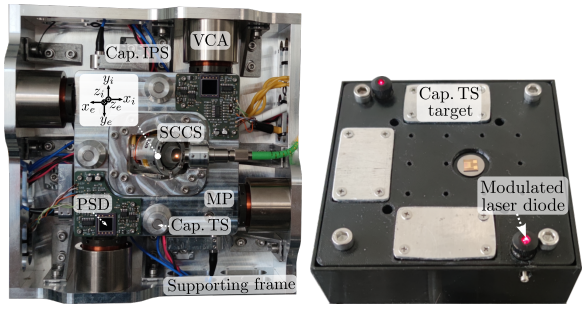

(a) Measurement module. (b) Sample box.

Fig. 2: Setup enabling high precision sample-tracking. a) shows a detailed view of the sample-tracking measurement module. b) shows the sample box equipped with targets to enable the measurement of the out-of-plane and in-plane motion [15].

control error processing approach enabling feedback control of an industrial robot based on external sensor signals for integration in a dual-stage controlled 6-DoF tracking system. The concept and integrated design of the inline measurement system is introduced in Section II, followed by a description of the challenge of feedback-controlling an IR for dual-stage actuation concepts in Section III. Based on the identified problem, an advanced position error processing scheme is designed and implemented, that enables the long-range tracking of moving samples in Section IV. The sample-tracking performance is evaluated in Section V, while section VI concludes the paper.

II. Tracking of Moving Objects

In Fig. 1 the concept of a high-precision 3D inline measurement system is schematically illustrated. The measurement module is mounted as end effector to an IR. Its integrated MP embeds a SCCS as the 3D measurement tool (MT) and is capable of actively tracking the sample motion in 6-DOFs, e.g., maintaining a constant relative position. This enables the stiff link between the SCCS and the sample, by means of feedback control, enabling local lab-like conditions in vibration prone environments [18]. For this reason, the integrated tracking sensors (TSs) are used to measure the relative sample position ζ_e, i.e. x_e and z_e. A sample is placed on a conveyor system, with its velocity $v_S = v + \Delta v$ being a superposition of the process-induced conveyor velocity v and a disturbance-induced motion Δv. To maintain the MP platform within its limited actuation range, the IR's tool center point (TCP) is actively repositioned by the feedback controller $\mathbf{C_{IR}}$ based on the position ζ_i of the MP relative to the IR measured by the internal position sensors (IPSs). In this dual-stage actuation concept, the MP is the high-precision actuator with a short actuation range and the IR provides the long-range coarse positioning, enabling high-precision 3D measurements on moving objects.

A. Active sample-tracking measurement platform

The integrated MP is magnetically levitated by eight identical voice coil actuators (VCAs) to enable quasi-zero stiffness actuation in six DOFs and to decouple it from disturbances induced by the limited positioning precision of the IR [15]. The actuation range is about $\pm 175\,\mu\mathrm{m}$ and $\pm 3\,\mathrm{mrad}$ in the translational and rotational DOFs, respectively. To measure the MP's position relative to the IR six capacitive IPSs are used. Based on the measured MP position the IR is repositioned by the controller $\mathbf{C_{IR}}$, see Fig. 1. The relative in-plane position between the sample and the MP is measured by two position sensitive detectors (PSDs), while the out-of-plane position is obtained by integrating three capacitive TSs. High-precision 3D measurements are enabled by a SCCS, achieving a lateral and axial resolution of $2.5\,\mu\mathrm{m}$ and $77\,\mathrm{nm}$, respectively [16].

The positioning uncertainty of the feedback-controlled MP is about $25\,\mathrm{nm}$ rms in the translational out-of-plane (z) and about $200\,\mathrm{nm}$ rms in the translational in-plane DOFs (x and y). The sample box shown in Fig. 2b is used as carrier of the sample to be inspected. It integrates aluminum targets for the capacitive sensors and modulated laser diodes as markers for the PSDs

B. Industrial robot and conveying system

The sample-tracking 3D measurement module (see Fig. 2a) is mounted as end effector to the IR (KUKA KR 10 R900-2, KUKA AG, Augsburg Germany), as shown in Fig. 3. The sample box introduced in Section II-A is placed on the sledge of a linear stage, emulating an industrial production line. As shown in Fig. 3, the IR's pose is adjusted such that the tracking sensors of the MP are aligned with respect to the sample surface, enabling an active tracking of the sample motion in six DOFs. Since the internal parameters of the KUKA KR 10 R900-2 are not accessible, it is not possible to design advanced

Pre-print version of the article: M. Laimer, D. Wertjanz, P. Gsellmann, G. Schitter, and E. Csencsics, "Enabling feedback position control of an industrial robot based on external sensor signals for dual-stage actuation," *2024 IEEE International Conference on Advanced Intelligent Mechatronics (AIM)*1252-1257, 2024. DOI: 10.1109/AIM55361.2024.10637010

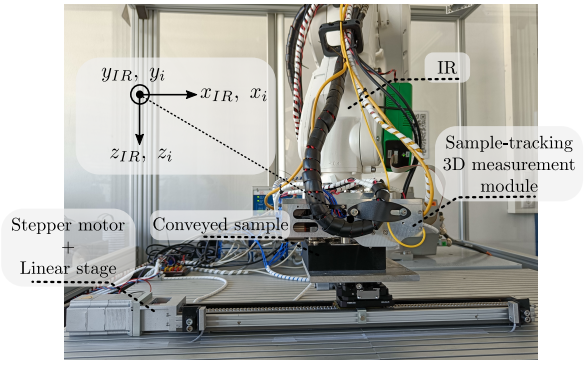

Fig. 3: Experimental setup of the dual stage positioning system for high-precision 3D measurements on moving samples. The long-range motion of the sample being conveyed by the linear stage is actively tracked using a dual stage control structure.

control strategies, such as computed torque concepts [19], to reposition the IR based on external sensor signals. For this reason the supplementary package robot sensor interface (RSI, KUKA AG, Augsburg Germany) [20] is used, which allows to reposition the IR's TCP in cartesian coordinates based on cyclically transmitted correction values. A more detailed description of this interface is given in Section III.

As discussed in Section II, the IR is repositioned according to the internal MP position errors, in order to maintain the MP within its limited actuation range, while actively tracking a sample motion.

III. System analysis

To actively track a moving sample with sub-micrometer precision along arbitrary paths, the IR needs to be continuously repositioned such that the sample-tracking platform is maintained within its actuation range. Since the motion range of the sample-tracking platform is $\pm 175\,\mu m$ for the translational DOFs, the IR's end effector position needs to be precisely controlled. As the disturbing sample motion is typically not known in advance, standard IR control concepts, such as off- or online path planning, are not suitable, requiring feedback control strategies instead.

KUKA provides the Robot Sensor Interface (RSI) [20] to reposition the IR's TCP based on cyclically transmitted correction values. The cycle time of the RSI is $4\,ms$. In addition, the RSI enables to connect external sensors or programmable logic controls (PLCs) via EtherCAT to the control unit of the IR. The typical communication structure of the RSI is shown in Fig. 4.

The in- and output bits can be grouped to define different datatypes, such as a BOOL, consisting of 8 Bit or a DWORD taking 32 Bit, which can then be connected to the I/Os of the RSI context. A RSI context defines the actual procedure, how the IR's TCP is replaced based on the external input signals. The IR's TCP can be repositioned absolute or relative, as shown in Fig. 5.

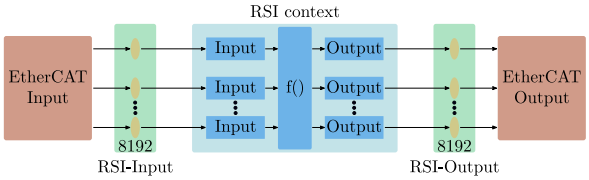

Fig. 4: The communication structure of the RSI. The EtherCAT in- and outputs enable to connect external sensors and PLCs to the control unit of the IR. The RSI context defines the procedure, of how the IR's TCP is repositioned based on external signals.

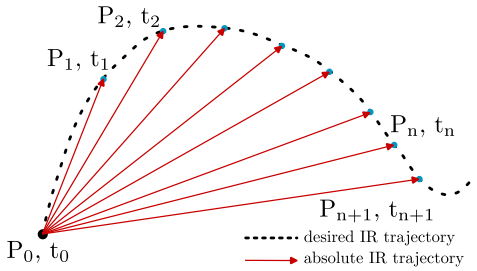

(a) Absolute IR trajectory.

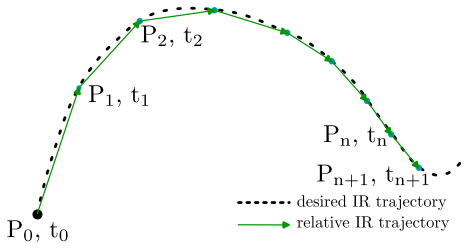

(b) Relative IR trajectory.

Fig. 5: Absolute and relative motion correction of the IR's TCP based on external signals. a) shows the procedure to reach a new point along a desired trajectory in absolute coordinates. b) shows how the IR's TCP is repositioned relatively to follow a trajectory.

Starting from an initial point P_0, a Point P_n in absolute coordinates can be reached by calculating its distance $d_{\overline{P_n P_0}}$ to the origin P_0. Repeating this step for every point (P_1 ... P_n), the IR's TCP can follow a trajectory guided by external input signals, as shown in Fig. 5a. To follow a trajectory relatively (Fig. 5b), the IR's motion is defined by the distance from point P_n to the next point P_{n+1}. As the location of the sample-tracking platform is measured relative to the IR's end effector position, the RSI relative motion correction is used to reposition the IR's TCP accordingly. To analyze, how the received correction values are processed by the RSI, a relative correction value of $10\,\mu m$ is transmitted over one and two cycles in the DOF x, respectively. The response of the robot is shown in Fig. 6. A correction value of $10\,\mu m$ is

Pre-print version of the article: M. Laimer, D. Wertjanz, P. Gsellmann, G. Schitter, and E. Csencsics, "Enabling feedback position control of an industrial robot based on external sensor signals for dual-stage actuation," *2024 IEEE International Conference on Advanced Intelligent Mechatronics (AIM)*1252-1257, 2024. DOI: 10.1109/AIM55361.2024.10637010

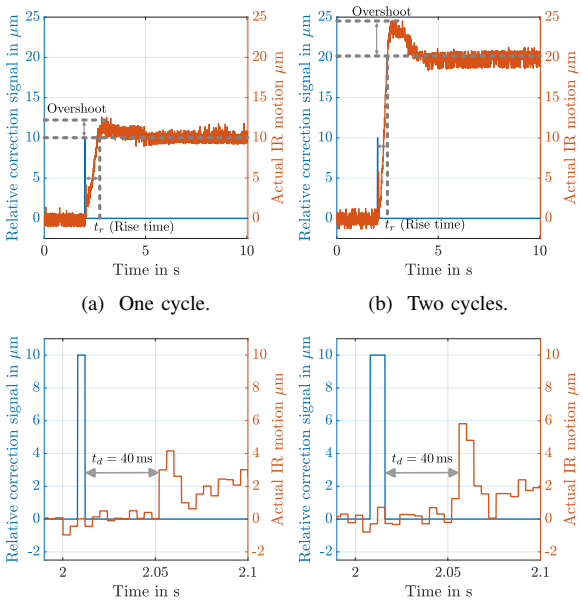

(a) One cycle. (b) Two cycles.

(c) One cycle zoomed. (d) Two cycles zoomed.

Fig. 6: Measured IR position for a correction value of 10 µm applied to the RSI in DOF x. a) and b) show the total IR motion for the correction value being transmitted over one and two communication cycles, respectively. The transmitted correction value is internally queued by the RSI, if applied over several cycles. A delay time of 40 ms is identified in c) and d).

applied for one cycle. It shows that the rise time t_r is 0.6 s with an overshoot of roughly 20 %. A similar behavior can be recognized, when the correction value is applied for two cycles. The IR is repositioned by 20 µm in total with a rise time of 0.5 s and an overshoot of 20 %. An overall motion of 20 µm when applying a correction value over two cycles suggests that the RSI is internally queuing the transmitted correction values. As shown in Fig. 6c and 6d, a delay time T_d of 40 ms is identified. Considering both, the internal queuing of the transmitted correction values and the delay time of the system, it is not possible to directly apply the internal position errors of the sample-tracking platform to the RSI, for repositioning the IR's TCP. If for example the sample-tracking platform is displaced by 15 µm from its center position in DOF x, the overall motion performed by the IR would be 150 µm, due to the delay time of the system and the queuing of the transmitted correction values. Taking also an overshoot of 20 % into account, the IR would move by 180 µm in x-direction, exceeding the overall actuation range of the MP, which my cause severe damage.

IV. Advanced Position Error Processing

This section provides a more detailed description of the implemented dual-stage control (see Fig. 7). Based on the findings in the previous Section IV, the internal position error signal cannot be directly applied to the RSI to reposition the IR's TCP. To enable the control of the IR to maintain the sample-tracking platform within its actuation range, the control structure is developed in the following.

Within the light-red box in Fig. 7, the control to reposition the IR's TCP is illustrated. Based on the measured internal position error $\mathbf{e}_{\zeta,\mathbf{i}}$ of the sample tracking platform, a delta error $\mathbf{\Delta e}_{\zeta,\mathbf{i}} = \mathbf{e}_{\zeta,\mathbf{i}} - \mathbf{e}_{\zeta,\mathbf{i-1}}$ of the internal position is defined. By introducing the delta error $\mathbf{\Delta e}_{\zeta,\mathbf{i}}$, the disadvantageous behavior described by Fig. 6 can be avoided, since only the change of the internal MP position error is transmitted. However, by implementing this strategy the information of the internal reference positions $\zeta_{\mathbf{i,r}}$ is lost. To keep the overall internal position error of the sample-tracking platform close to zero (reference position), an additional integrator in the form of a lowpass filter is introduced. The error signals $\mathbf{e}_{\zeta,\mathbf{i}}$ are averaged by a lowpass filter with a 3 dB cut-off frequency of 10 Hz, resulting in $\overline{\mathbf{e}}_{\zeta,\mathbf{i}}$. If the averaged internal MP position error $\overline{\mathbf{e}}_{\zeta,\mathbf{i}}$ exceeds a defined tolerance $tol_{\overline{e}}$ of 10 µm and 40 µrad for the translational and rotational DOFs, respectively, the error signal $\overline{\mathbf{e}}_{\zeta,\mathbf{i}}$ is added to the delta error $\mathbf{\Delta e}_{\zeta,\mathbf{i}}$ for one cycle, resulting in $\tilde{\mathbf{e}}_{\zeta,\mathbf{i}} = \mathbf{\Delta e}_{\zeta,\mathbf{i}} + \overline{\mathbf{e}}_{\zeta,\mathbf{i-1}}$. After adding the averaged error $\overline{\mathbf{e}}_{\zeta,\mathbf{i}}$ for one cycle, a sufficient time delay is applied, before adding the average distance to the internal reference positions $\zeta_{\mathbf{i,r}}$ again. This is required to avoid the effect of internally queuing, as described in III. The resulting error signal $\tilde{\mathbf{e}}_{\zeta,\mathbf{i}}$ is applied as input to the PI position control [17]

$$u_{IR}(k) = k_p\left(\tilde{e}_{\zeta,i}(k) + \frac{T_s}{T_i}\sum_{l=0}^{k}\tilde{e}_{\zeta,i}(l)\right). \tag{1}$$

Based on the measured IR dynamics, the control parameters for each DOF are identified in a loop-shape approach. For the DOF x, which requires the highest IR control effort, due to sample motion direction (see Fig. 3), a robust gain and phase margin of 14 dB and 45° for a cross-over frequency of 0.55 Hz are achieved. To further improve the tracking performance, the conveyor velocity can be considered in a feedforward control additionally. Therefore, the output $\mathbf{u_{IR,FB}}$ of the controller $\mathbf{C_{IR}}$ is superimposed with the feedforward output $\mathbf{u_{IR,FF}}$ of the conveyor velocity v. The parameter $\mathbf{k_v}$ converts the velocity signal into a corresponding position signal for one RSI communication cycle. The detailed discussion of the IR dynamics identification and control design for the other DOFs is given in [17].

Within the light-gray box, the control structure of the MP is illustrated. The tracking error $\tilde{\mathbf{e}}_{\zeta,\mathbf{e}}$ is used as input of the 6-DOF PID controller $\mathbf{C_{MP}}$. The PID control parameters are chosen to achieve cross-over frequencies of 300 Hz with gain margins of at least 10 dB and phase margins above 30° for all six DOFs. The output of the controller is applied to the voice coil-actuated system [15].

Pre-print version of the article: M. Laimer, D. Wertjanz, P. Gsellmann, G. Schitter, and E. Csencsics, "Enabling feedback position control of an industrial robot based on external sensor signals for dual-stage actuation," *2024 IEEE International Conference on Advanced Intelligent Mechatronics (AIM)*1252-1257, 2024. DOI: 10.1109/AIM55361.2024.10637010

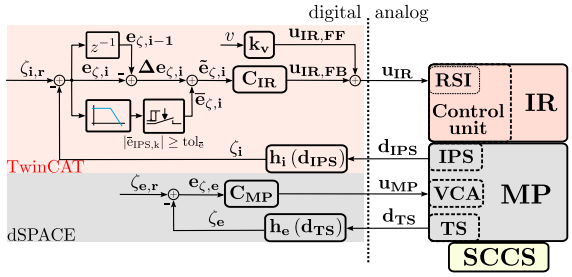

Fig. 7: Block diagram of the dual stage-controlled robotic 3D measurement system. The SCCS is positioned relative to a sample by the feedback controller $\mathbf{C_{MP}}$. Based on the measured internal MP position and an advanced error processing approach is implemented to enable a feedback control $\mathbf{C_{IR}}$ of the IR based on the measured internal MP position error to maintain the MP within its limited actuation range.

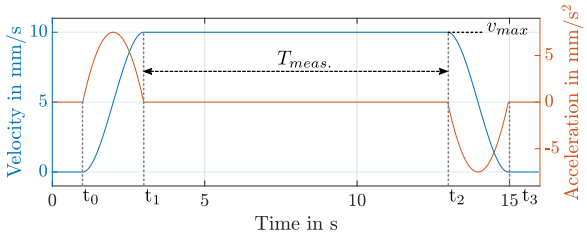

Fig. 8: Sample velocity trajectory. Within the time interval $[t_0, t_1]$, the sample is accelerated from zero to a targeted velocity v_{max}. The sample velocity is kept constant for 10 s during the interval $T_{meas.} = [t_1, t_2]$ before it gets decelerated back to zero during the interval $[t_2, t_3]$.

V. Experimental Performance Evaluation

Since the IR cannot be repositioned without the introduced advanced position error processing, this section aims to demonstrate the tracking performance of the derived system for samples placed on a conveying system.

As introduced in Section II-A, the sample is accelerated along the x-axis according to the acceleration profile as shown in Fig 8. A maximum velocity of $v_{max} = 10\,\mathrm{mm\,s^{-1}}$ is reached, after an acceleration phase $[t_0, t_1]$ of 2 s. Within $T_{meas} = [t_0, t_1]$, the sample velocity is kept constant for 10 s. This time interval serves as a time slot to perform the actual 3D measurements on the sample [17], as well as to evaluate the sample-tracking performance of the dual-stage controlled robotic tracking system. As performance measures, the RMS value of the internal MP position error and the tracking errors are considered. For the internal MP position errors, a value close to zero indicates that the MP remains near its center position, providing its major actuation range for tracking sample motions induced by higher-frequency disturbances. The performed motion of the IR in the DOF x and z as well as the internal MP position error for both DOFs are shown in Fig. 9. In sample motion direction, the internal MP position error is 17.5 µm rms. This indicates that almost 90 % of the MP's actuation range remains for compensating higher frequent sample motion. For the out-of-plane DOF z, the internal MP position error is 13.5 µm rms, performing slightly better compared to the motion direction x. Within the time interval $T_{meas} = [t_0, t_1]$ it is decisive, that the sample-tracking error is kept as low as possible, to establish local lab-like conditions for the measurement tool.

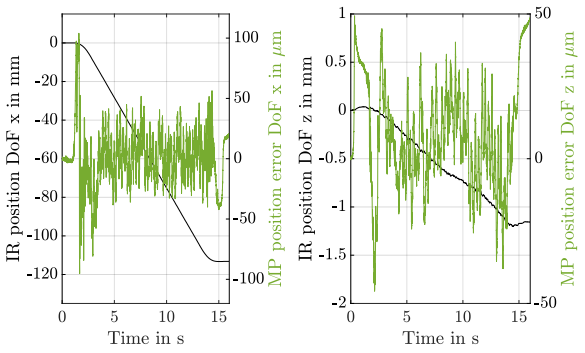

(a) DoF x. (b) DoF z.

Fig. 9: Evaluated performance of the IR repositioning in 6-DOFs based on the internal MP position error signals for the performed target motion trajectory of Fig. 8. a) shows the performed IR motion with the according internal MP position error in DOF x. b) shows the performed IR motion with the according internal MP position error in DOF z.

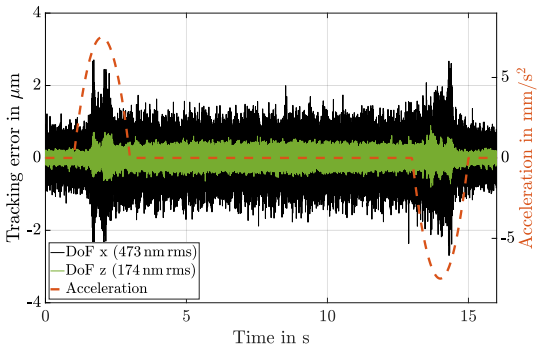

Fig. 10: Evaluated sample tracking performance for the in-plane DOF x and the out-of-plane DOF z for the performed target motion trajectory of Fig. 8. The acceleration trajectory indicates that the tracking error is highest during the acceleration and deceleration of the sample.

The residual sample-tracking error along the motion direction x and the out-of-plane DOF z are shown in Fig. 10. For a constant velocity $v = 10\,\mathrm{mm\,s^{-1}}$, residual sample-tracking

Pre-print version of the article: M. Laimer, D. Wertjanz, P. Gsellmann, G. Schitter, and E. Csencsics, "Enabling feedback position control of an industrial robot based on external sensor signals for dual-stage actuation," *2024 IEEE International Conference on Advanced Intelligent Mechatronics (AIM)*1252-1257, 2024. DOI: 10.1109/AIM55361.2024.10637010

errors below 500 nm rms and 200 nm rms are achieved in the translational in- and out-of-plane DOFs. The deviation in the tracking performance can be explained by the different sensing principles and the related noise floors of the in- and out-of-plane TSs (see Section II-B) [21].

In summary, the proposed advanced error processing strategy enables the feedback control of the IR based on the internal MP position errors. It can be shown that during the active tracking of the sample, more than 90 % of the MP's actuation range is available for cancelling higher frequent sample disturbances. With tracking errors on the order of 500 nm rms and 200 nm rms for the translational DOF x and z, it clearly demonstrates the capability of tracking a sample with sub-micrometer precision.

VI. Conclusion

This paper presents a feedback position controlled IR based on external sensor signals for dual-stage actuation concepts. A high-precision measurement module is mounted as end effector to the IR, providing the short-stroke but high-precision positioning of a 3D measurement tool relative to a sample surface in 6-DoF. To reposition the IR based on the internal MP position errors, the RSI from KUKA is used, enabling a sensor guided positioning of the IR's TCP. Due to the identified delay time of the system and as a result the queuing of applied correction values, an advanced position error processing strategy has been introduced. With this concept, only the change of the internal MP position error is transmitted to the RSI, enabling the position feedback control of the IR's TCP, to maintain the MP within its actuation range. Experimental results demonstrate the effectiveness of the proposed concept, with more than 90 % of the MP's actuation range remaining to track higher frequent sample motion for conveying velocities up to 10 mm s^{-1}. In addition, a sample-tracking performance of 500 nm rms and 200 nm rms for the translational DOF x and z clearly demonstrate the effective establishment of local lab-like conditions in vibration prone environments.

Acknowledgment

The financial support by the Austrian Federal Ministry of Labour and Economy, the National Foundation for Research, Technology and Development and the Christian Doppler Research Association, and Micro-Epsilon Atensor GmbH and MICRO-EPSILON-MESSTECHNIK GmbH & Co.K.G. is gratefully acknowledged. This project is partially funded by the Hochschuljubilaeumsfonds of the city of Vienna, Austria under the project number H-260744/2020.

References

[1] D. Imkamp, R. Schmitt, and J. Berthold, "Blick in die Zukunft der Fertigungsmesstechnik," vol. 79, no. 10, pp. 433–439, 2012.

[2] D. Imkamp, J. Berthold, M. Heizmann, K. Kniel, M. Peterek, R. Schmitt, J. Seidler, and K.-D. Sommer, "Herausforderungen und Trends in der Fertigungsmesstechnik – Industrie 4.0," *tm - Technisches Messen*, vol. 83, no. 7-8, pp. 417–429, 2016.

[3] H. Lasi, P. Fettke, H.-G. Kemper, T. Feld, and M. Hoffmann, "Industry 4.0," *Business & information systems engineering*, vol. 6, no. 4, pp. 239–242, 2014.

[4] R. Schmitt and F. Moenning, "Ensure success with inline-metrology," in *XVIII IMEKO World Congress - Metrology for a Sustainable Development*, 2006.

[5] I. Iglesias, M. Sebastián, and J. Ares, "Overview of the state of robotic machining: Current situation and future potential," *Procedia Engineering*, vol. 132, pp. 911–917, 2015, mESIC Manufacturing Engineering Society International Conference 2015.

[6] M. Bartoš, V. Bulej, M. Bohušík, J. Stanček, V. Ivanov, and P. Macek, "An overview of robot applications in automotive industry," *Transportation Research Procedia*, vol. 55, pp. 837–844, 2021, 14th International scientific conference on sustainable, modern and safe transport.

[7] W. Ji and L. Wang, "Industrial robotic machining: A review," *International Journal of Advanced Manufacturing Technology*, vol. 103, pp. 1239–1255, 07 2019.

[8] F. Berry, R. Mermet-Lyaudoz, J. M. Cuevas Davila, D. A. Djemmah, H. S. Nguyen, C. Seassal, E. Fourmond, C. Chevalier, M. Amara, and E. Drouard, "Light management in perovskite photovoltaic solar cells: A perspective," *Advanced Energy Materials*, vol. 12, no. 20, p. 2200505, 2022.

[9] M. Liebens, A. Jourdain, J. De Vos, T. Vandeweyer, A. Miller, E. Beyne, S. Li, G. Bast, M. Stoerring, S. Hiebert, and A. Cross, "In-line metrology for characterization and control of extreme wafer thinning of bonded wafers," *IEEE Transactions on Semiconductor Manufacturing*, vol. 32, no. 1, pp. 54–61, 2019.

[10] B. Bessason and C. Madshus, "Evaluation of site vibrations for metrology laboratories," *Measurement Science and Technology*, vol. 11, no. 10, p. 1527, 2000.

[11] M. Thier, R. Saathof, R. Hainisch, and G. Schitter, "Vibration compensation platform for robot-based nanoscale measurements," in *15th International Conference of the European Society for Precision Engineering and Nanotechnology, EUSPEN 2015*, pp. 211–212. EUSPEN, 2015.

[12] S. Lemes, D. Strbac, and M. Cabaravdic, "Using industrial robots to manipulate the measured object in CMM," *International Journal of Advanced Robotic Systems*, vol. 10, no. 7, p. 281, 2013.

[13] E. Csencsics, M. Thier, S. Ito, and G. Schitter, "Supplemental peak filters for advanced disturbance rejection on a high precision endeffector for robot-based inline metrology," *IEEE/ASME Transactions on Mechatronics*, p. 1, 2021.

[14] M. Thier, R. Saathof, A. Sinn, R. Hainisch, and G. Schitter, "Six degree of freedom vibration isolation platform for in-line nano-metrology," *IFAC-PapersOnLine*, vol. 49, no. 21, pp. 149–156, 2016.

[15] D. Wertjanz, E. Csencsics, T. Kern, and G. Schitter, "Bringing the lab to the fab: Robot-based inline measurement system for precise 3-D surface inspection in vibrational environments," *IEEE Transactions on Industrial Electronics*, vol. 69, no. 10, pp. 10 666–10 673, 2022.

[16] D. Wertjanz, T. Kern, E. Csencsics, G. Stadler, and G. Schitter, "Compact scanning confocal chromatic sensor enabling precision 3-D measurements," *Applied Optics*, vol. 60, no. 25, pp. 7511–7517, Sep. 2021.

[17] M. Laimer, D. Wertjanz, P. Gsellmann, G. Schitter, and E. Csencsics, "High-precision 3d measurements on moving objects," *IEEE Transactions on Mechatronics*, 2023 (under review).

[18] D. Wertjanz, E. Csencsics, and G. Schitter, "Three-DoF vibration compensation platform for robot-based precision inline measurements on free-form surfaces," *IEEE Transactions on Industrial Electronics*, vol. 69, no. 1, pp. 613–621, 2022.

[19] D. Nguyen-Tuong, M. Seeger, and J. Peters, "Computed torque control with nonparametric regression models," in *2008 American Control Conference*, pp. 212–217. IEEE, 2008.

[20] KUKA Deutschland GmbH, "KUKA.RobotSensorInterface 4.1," https://xpert.kuka.com/service-express/portal/project1_p/document/kuka-project1_p-common_PB11890_de?context=%7B%7D, accessed: 18.01.2024.

[21] D. Wertjanz, E. Csencsics, and G. Schitter, "An efficient control transition scheme between stabilization and tracking task of a MAGLEV platform enabling active vibration compensation," in *2020 IEEE/ASME International Conference on Advanced Intelligent Mechatronics (AIM)*, pp. 1943–1948, 2020.

Pre-print version of the article: M. Laimer, D. Wertjanz, P. Gsellmann, G. Schitter, and E. Csencsics, "Enabling feedback position control of an industrial robot based on external sensor signals for dual-stage actuation," *2024 IEEE International Conference on Advanced Intelligent Mechatronics (AIM)*1252-1257, 2024. DOI: 10.1109/AIM55361.2024.10637010